RSC Advances

REVIEW

View Article Online
View Journal | View Issue

Cite this: *RSC Adv.*, 2017, **7**, 50195

High-pressure synthesis, crystal structure and photoluminescence properties of a new terbium silicate: $Na_2Tb_{1.08}Ca_{2.92}Si_6O_{18}H_{0.8}$†

Xinjian Bao,[abc] Xiaoyang Liu [c] and Xi Liu *[ab]

The crystal properties of a terbium silicate $Na_2Tb_{1.08}Ca_{2.92}Si_6O_{18}H_{0.8}$ synthesized at 1 GPa and 800 °C using a piston-cylinder apparatus is reported. Our single-crystal X-ray analysis shows that this new compound is triclinic with the space group $P\bar{1}$ ($Z = 1$), and its unit-cell parameters are $a = 7.056(3)$ Å, $b = 7.075(3)$ Å, $c = 8.029(3)$ Å, $\alpha = 102.381(5)°$, $\beta = 95.387(6)°$, $\gamma = 90.552(6)°$, and $V = 389.6(2)$ Å^3. This structure consists of octahedral double chains of the compositions $[Ca_{0.875}Tb_{0.125}O_6]$ and $[Ca_{0.585}Tb_{0.415}O_6]$. The double chains are linked by tetrasilicate chains *via* vertex oxygen atoms to form a 3D framework with 6-membered (2 octahedra and 4 tetrahedra) ring channels along the *b*-axis where the Na^+ cations locate. The luminescence properties of the $Na_2Tb_{1.08}Ca_{2.92}Si_6O_{18}H_{0.8}$ phase are also investigated. This phase, with most of its Tb in 3+, emits mainly from one transition, $^5D_4 \rightarrow {}^7F_5$ (542 and 552 nm). The room temperature fluorescence decay curves are fit well by an exponential function, yielding a lifetime value of about 2.498(7) ms.

Received 13th September 2017
Accepted 23rd October 2017

DOI: 10.1039/c7ra10182a

rsc.li/rsc-advances

1. Introduction

Microporous lanthanide-containing silicates constitute a novel family of zeotype materials made of interlinked octahedra and tetrahedra. Many studies have focused on the synthesis of this group of compounds for their versatility in terms of chemical compositions, framework topologies and ion-exchange properties, as well as their interesting physical and chemical properties.[1–5] Due to their high thermal stability and tunable optical properties, the lanthanide-containing silicates attract much interest as candidates of optical materials.[6–8] In 1997, Rocha *et al.* reported a microporous sodium yttrium silicate $Na_4K_2Y_2Si_{16}O_{38}\cdot 10H_2O$.[9] Since then a series of microporous lanthanide silicates have been successfully prepared. Recently, many studies have focused on the possibility to obtain phosphors with emission across the entire visible range by selection of lanthanide ions.[10–13]

High-pressure (HP) experimental techniques have been usually employed in synthesizing the lanthanide-containing silicates in recent decades. As a few examples, Huang *et al.* documented the HP synthesis of a new europium silicate $Cs_3EuSi_6O_{15}$, which consists of loop-branched vierer double chains of silicate with four-, six-, and eight-membered rings;[3] Zhao *et al.* reported the HP synthesis of three new lanthanide silicates based on anionic silicate chain, layer, and framework.[14] Liu's group synthesized a number of lanthanide-containing silicates under HP conditions and reported their structural features.[15–18]

In this work a new terbium silicate, $Na_2Tb_{1.08}Ca_{2.92}Si_6O_{18}H_{0.8}$, was synthesized at HP condition using a piston-cylinder apparatus. The crystallographic details of this phase were obtained by performing single-crystal X-ray diffraction analysis, and the luminescence properties were systematically investigated using a range of analytical techniques as well.

2. Experiment

2.1. Synthesis

The starting material was made as following: pure chemicals $NaOH\cdot H_2O$ (Alfa Aesar, powder, 99.9%), $TbCl_3\cdot 6H_2O$ (Alfa Aesar, powder, 99.9%), $CaCO_3$ (Alfa Aesar, powder, 99.9%) and SiO_2 (Alfa Aesar, powder, 99.9%) were weighed without any pretreatment, ground and homogenized in an agate mortar. This mixture was subsequently stored in a drying oven at 110 °C for later synthesizing experiment. The molar ratio of these chemicals in the starting material was ideally $NaOH\cdot H_2O : TbCl_3\cdot 6H_2O : CaCO_3 : SiO_2 = 2 : 1 : 3 : 6$, leading to ~11.9 wt% CO_2 and 11.32 wt% H_2O in the bulk composition. The starting material was loaded into a Pt capsule, which was sealed at both ends using an arc-welding technique. Our synthesizing experiment was carried out with a piston-cylinder apparatus (Depths of The Earth Company Quickpress[19,20]). The experimental assembly and high-P experimental technique were

[a]*Key Laboratory of Orogenic Belts and Crustal Evolution, MOE, Peking University, Beijing 100871, China. E-mail: xi.liu@pku.edu.cn; Fax: +86-10-6275-2996; Tel: +86-10-6275-3585*

[b]*School of Earth and Space Sciences, Peking University, Beijing 100871, China*

[c]*State Key Laboratory of Inorganic Synthesis and Preparative Chemistry, College of Chemistry, Jilin University, Changchun 130012, China*

† Electronic supplementary information (ESI) available. CCDC 1574110. For ESI and crystallographic data in CIF or other electronic format see DOI: 10.1039/c7ra10182a

generally identical to those reported in.[21] Our sample was synthesized at 1 GPa and 800 °C with a heating time of 24 hours. After the reaction, the sample was quickly cooled down to room temperature by switching off the electrical power supply. Some parts of the resulting sample were first crushed, then treated with diluted HCl to remove any possible residues of carbonate and hydrate, and finally washed with deionized water for further test.

2.2. Characterizations

Powder X-ray diffraction (XRD) data were collected using a Rigaku D/Max 2550 V/PC X-ray diffractometer with graphite-monochromated Cu Kα radiation (λ = 0.15418 nm) at 50 kV and 200 mA at room temperature. Energy-dispersive spectroscopy (EDS) analysis was carried out using an EDS system attached to a JEOL JXA-8100 electron microprobe. The instrument was calibrated using a series of standards from Structure Probe, Inc. XPS valence band spectra were obtained with an ESCA LAB 250 photoelectron spectrometer. IR spectrum was recorded on a Nicolet Impact 410 FT-IR spectrometer using the KBr pellet technique. Thermogravimetric analysis (TG) was carried out on a Perkin-Elmer TGA unit in air with a heating rate of 10 °C min^{-1}. Photoluminescence (PL) spectra were obtained on a F7000 (Hitachi) spectrophotometer with Xe 900 (150 W xenon arc lamp) as the light source. PL decay curves were measured on an FLS980 spectrophotometer (Edinburgh Instruments) with an mF90H flash lamp as the light source. To eliminate the second-order emission from the source radiation, a cut-off filter was used during the measurement. Slit widths were 0.20 (excitation) and 0.20 (emission) nm. All spectra were recorded at room temperature.

2.3. Single-crystal X-ray diffraction

Suitable single crystal was selected for single-crystal X-ray diffraction analysis. Intensity data was collected on a Bruker Smart ApexII Quazar micro-focused diffractometer using Mo Kα radiation (λ = 0.71073 nm). The raw data was processed and corrected for the absorption effects using SAINT$^+$ and SADAB. An initial structure solution was obtained *via* direct methods and refined by a full-matrix least-squares method using the SHELXT software included in the SHELXTL package. All heavy atoms (Na, Tb, Ca, and Si) were first located unambiguously in the Fourier maps, and then the O atoms were found in the subsequent difference maps. All atoms were refined with anisotropic displacement parameters. The final cycles of the least-squares refinement including atomic coordinates and anisotropic thermal parameters for the atoms [$I > 2\mathrm{sigma}(I)$] converged at $R_1 = 0.0502$, w$R_2 = 0.1186$, and $S = 1.015$ for this new terbium silicate compound.

3. Results and discussion

3.1. Phases in synthetic material

The SEM backscatter image shown in Fig. S1† indicates that there is just one crystalline phase in our synthetic product, in good agreement with our powder XRD data. The powder XRD pattern of the experimental product is shown in Fig. 1; since it is completely consistent with the simulated XRD pattern based on our single-crystal structure data (to be reported in the next Section), one crystalline phase in the experimental product is the only possible explanation. In addition, Fig. S1† reveals significant amount of holes and cracks in the sample, suggesting the role of a C–H–O fluid phase in our experiment; note that there was ~23.22 wt% CO_2 and H_2O in the starting material. Ten EDS analyses performed on arbitrarily selected areas of the experimental product suggest a cation ration of Na : Tb : Ca : Si = 2 : 1.08 : 2.92 : 6, slightly different from the original and ideal cation ration of Na : Tb : Ca : Si = 2 : 1 : 3 : 6 in the bulk composition. This compositional difference partially reflects a possible drawback of using untreated chemicals to

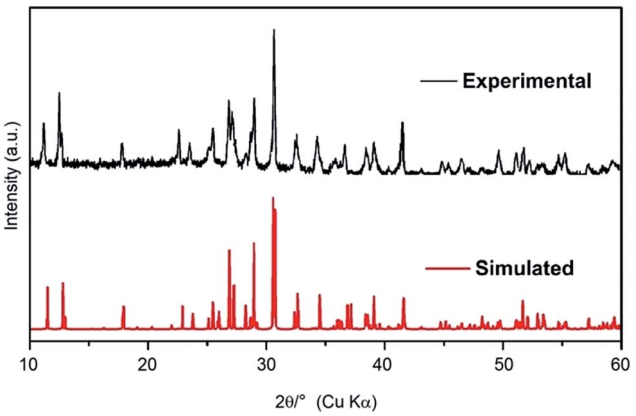

Fig. 1 Experimental and simulated powder X-ray diffraction patterns of the $Na_2Tb_{1.08}Ca_{2.92}Si_6O_{18}H_{0.8}$ compound. The simulated pattern is based on the structure refined by our single-crystal X-ray diffraction analysis.

Table 1 Crystal data and structure refinement for the $Na_2Tb_{1.08}Ca_{2.92}Si_6O_{18}H_{0.8}$ compound

Empirical formula	$Na_2Tb_{1.08}Ca_{2.92}Si_6O_{18}H_{0.8}$	
Formula weight	792.01	
Temperature	296(2) K	
Wavelength	0.71073 Å	
Crystal system, space group	Triclinic, $P\bar{1}$	
Unit cell dimensions	a = 7.056(3) Å	α = 102.381(5)°
	b = 7.075(3) Å	β = 95.387(6)°
	c = 8.029(3) Å	γ = 90.552(6)°
Volume	389.6(2) Å^3	
Z	1	
Crystal size	0.1 × 0.08 × 0.08 mm	
Theta range for data collection	2.61–25.34°	
Limiting indices	$-3 \le h \le 8$, $-8 \le k \le 8$, $-9 \le l \le 9$	
Reflections collected/unique	2059/1416 [R(int) = 0.0109]	
Completeness to theta = 25.10	99.20%	
Refinement method	Full-matrix least-squares on F^2	
Data/restraints/parameters	1416/1/141	
Goodness-of-fit on F^2	1.015	
Final R indices [$I > 2\mathrm{sigma}(I)$]	R_1 = 0.0502, wR_2 = 0.1186	
R Indices (all data)	R_1 = 0.0506, wR_2 = 0.1188	
Largest diff. Peak and hole	0.898 and −0.978e Å^{-3}	

prepare the starting material, and partially implies that the C–H–O fluid was not pure, but dissolved some Na, Ca and Si.

Combined with the single-crystal structure data, XPS data, FT-IR data and TG data reported below, the composition of this crystalline phase has been approximated by the chemical formula of $Na_2Tb_{1.08}Ca_{2.92}Si_6O_{18}H_{0.8}$.

3.2. Single-crystal structure

The single-crystal analysis of the $Na_2Tb_{1.08}Ca_{2.92}Si_6O_{18}H_{0.8}$ silicate reveals that it crystallizes in the $\bar{P}1$ space group ($Z = 1$), with $a = 7.056(3)$ Å, $b = 7.075(3)$ Å, $c = 8.029(3)$ Å, $\alpha = 102.381(5)°$, $\beta = 95.387(6)°$, $\gamma = 90.552(6)°$, and $V = 389.6(2)$ Å^3 (Table 1). Each asymmetric unit of this new terbium silicate compound contains one distinct Na site, two distinct Ca(Tb) sites (denoted as M1 and M2), three distinct Si site and nine distinct O sites (Fig. S2†), with their coordinates and equivalent isotropic displacement parameters being listed in Table S1.†

This novel $Na_2Tb_{1.08}Ca_{2.92}Si_6O_{18}H_{0.8}$ compound has a 3D-framework structure (Fig. 2). Two distinct [MO_6] octahedra form edge-sharing double chains running along the *b*-axis. The [SiO_4] tetrahedron in the crystal structure is linked to two adjacent [SiO_4] tetrahedra, these three symmetrically independent [SiO_4] tetrahedra form a C-shaped cluster, and neighboring C-shaped clusters are linked *via* sharing O atoms to form a zigzag chain along the *b*-axis. The tetrahedral chain is linked to the double chains of the [MO_6] through corner-sharing. The stacking pattern along with the linkages between the layers of tetrahedra and octahedra gives rise to an I-beam topology where bands of the octahedra are linked to overlying and underlying silicate chains through the apical O atoms in the [SiO_4] tetrahedra. The resulting framework contains 4-membered and 6-membered ring channels along the *b*-axis, where the H and Na cations locate, respectively.

The Ca and Tb atoms are disordered over the M1 and M2 sites with different occupancies. In the M1 and M2 sites, the Ca occupancies are 0.875 and 0.585, respectively. The corresponding structural formula is thus $Na_2(Tb_{0.25}Ca_{1.75})(Tb_{0.83}Ca_{1.17})Si_6O_{18}H_{0.8}$. As shown in Fig. 2 and Table S2,† all the M sites are coordinated to six bridging O atoms to form [MO_6] octahedra. For the $M1O_6$, the lengths of the six M1–O bands lie between 2.295(8) to 2.491(8) Å while the O–M1–O angles from 79.4(3) to 167.9(3)°.

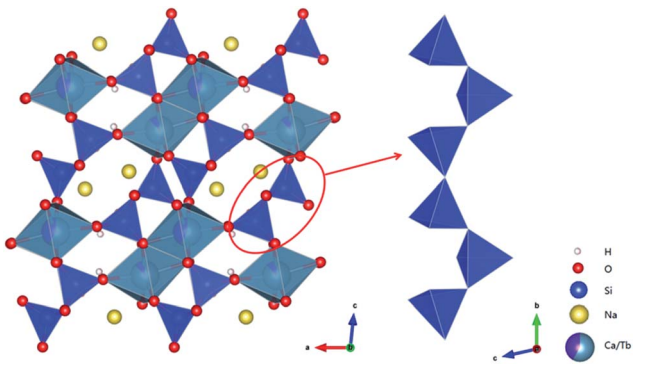

Fig. 2 Polyhedral view of the $Na_2Tb_{1.08}Ca_{2.92}Si_6O_{18}H_{0.8}$ compound along the *b*-axis and [SiO_4] tetrahedra single chain.

For the $M2O_6$, the M2–O band lengths are in the range from 2.281(7) to 2.474(8) Å while the O–M2–O angles from 80.8(3) to 176.6(3)°. The Tb atoms on these two sites have mixed valences, with the Tb^{3+} dominant: the XPS spectrum (Fig. S3†) shows two main peaks at ~148.11 and 150.27 eV, which are attributed to the Tb^{3+} and Tb^{4+}, respectively; the ratio of Tb^{4+} : Tb has been calculated as ~0.194 by performing peak-area analysis.[22] On the basis of charge balance, furthermore, the XPS data imply ~0.7 H in the unit cell of the crystal structure.

The Si atoms are all in 4-fold coordination, and form [SiO_4] tetrahedra. The Si–O lengths vary from 1.601(8) to 1.645(7) Å for the Si_1–O bonds, from 1.577(8) to 1.647(7) Å for the Si_2–O bonds, and from 1.593(7) to 1.666(7) Å for the Si_3–O bonds. The O–Si–O angles are shown in Table S2.†

The hydrogen site (H_1–O_1) has been confirmed by the electron density difference following the ref. 23,24. The hydrogen bond length was fixed as 0.84 Å during the refinement. In addition, the existence of the O–H bond has been confirmed by our IR analysis (Fig. S4†): the peaks at ~3500 cm^{-1} in the IR spectrum can be assigned to the O–H stretching bands. Further, the existence of the OH group in our new terbium silicate compound has been confirmed by the thermogravimetric analysis. As shown in Fig. S5,† the TG curve of the compound revealed a weight loss of ~1 wt% in the temperature range of ~300–650 °C. At temperatures higher than 650 °C, no significant weight loss occurred, indicating that the sample was almost anhydrous at relatively high temperatures. The TG data thus suggests approximately 0.88 H in the unit cell of this compound, a result in excellent agreement with that required by the XPS and EDS data if the experimental uncertainty in the TG analysis is taken into account.

With the knowledge of the cation–anion distances from Shannon,[25] the Na cation is coordinated to six O atoms with the Na–O bond lengths ranging from 2.295(8) to 2.502(8) Å. There are two more O atoms, with the distances of 2.967(9) and 2.991(9) Å, surrounding the Na atom as well.

Table S3† presents the calculated bond valence sums (BVSs).[26,27] The BVSs for the Si^{4+} cations are in good accordance with their theoretical values of 4.0 v.u. The total valences of the M cations are 9.2 v.u. depending on the formula, and the BVSs for the M cations are 9.376 v.u. which deviates slightly from the theoretical value by 1.02%. All O atoms show BVSs more or less close to their ideal values of 2.0 v.u. The relatively low values for O_1 (1.512 v.u.) and O_7 (1.618 v.u.) are explained by their connection to the H^+ cation. Taking into account the Tb occupation and BVSs of the M cations, the compositions of the cations on the M1 and M2 sites are tentatively determined as $Ca^{2+}_{0.875}Tb^{4+}_{0.125}$ and $Ca^{2+}_{0.585}Tb^{3+}_{0.415}$, respectively. With the cation radius data from Shannon,[25] the average cation radii of the M1 and M2 sites are calculated as 0.970 and 0.968 Å, respectively. It means that the coordination environments of the M1 and M2 sites are generally similar.

3.3. Photoluminescent studies

Fig. 3 shows the room temperature excitation spectra of the $Na_2Tb_{1.08}Ca_{2.92}Si_6O_{18}H_{0.8}$ phase, monitored within the

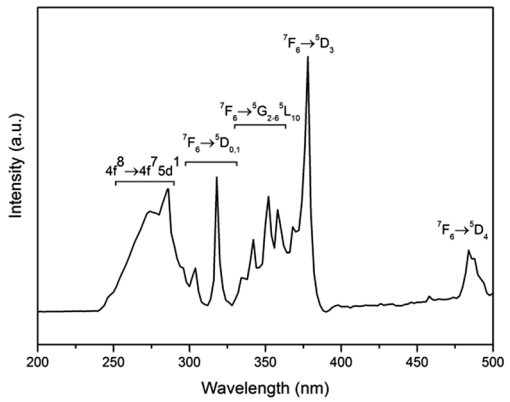

Fig. 3 Excitation spectrum of $Na_2Tb_{1.08}Ca_{2.92}Si_6O_{18}H_{0.8}$ (λ_{em} = 542 nm).

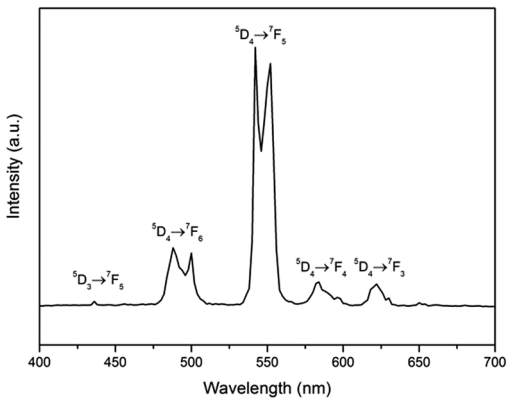

Fig. 4 RT emission spectra of $Na_2Tb_{1.08}Ca_{2.92}Si_6O_{18}H_{0.8}$ (λ_{em} = 378 nm).

Tb^{3+} $^5D_4 \rightarrow {}^7F_5$ transition (542 nm). In the excitation spectrum, the sharp lines between 320 and 500 nm are assigned as the intraconfigurational $4f^8$ transitions of the Tb^{3+} between the $^7F_6$ ground state and the $^5D_{0,1}$, $^5G_{2-6}$, $^5L_{10}$, and $^5D_{3,4}$ excited levels. On the other hand, the broad feature between ~240 and 320 nm may be contributed by both the spin-forbidden and spin-allowed interconfigurational $^4f_8 \rightarrow {}^4f_7{}^5d_1$ (f–d) transitions of the Tb^{3+};[28,29] specifically, the bands at ~275 nm can be assigned to the spin-allowed ^7D levels of the $4f^8 \rightarrow 4f^7 5d$ transition while the bands at ~300 nm can be assigned to the spin-forbidden ^9D levels of the $4f^8 \rightarrow 4f^7 5d$ transition of the Tb^{3+} ions.

Fig. 4 shows the RT emission spectrum of the $Na_2Tb_{1.08}Ca_{2.92}Si_6O_{18}H_{0.8}$ phase. The emission spectrum excited at 378 nm (Tb^{3+} $^5D_3$) displays a series of sharp lines from 475 to 675 nm, which are associated with the $^5D_4 \rightarrow {}^7F_{3-6}$ transitions of the Tb^{3+}, with the strongest at about 542 and 552 nm ($^5D_4 \rightarrow {}^7F_5$). No apparent emission from the Tb^{4+} ion is expected in this range due to the charge transfer.[30] Luminescence from any higher excited states (*e.g.*, $^5D_3$) is very weak. The peak at 436 nm is assigned to the transition $^5D_3 \rightarrow {}^7F_5$. Other potential emissions with origins from the $^5D_3$ to ^7F_j transitions of the Tb^{3+} ions are not detected due to the cross-relaxation effect.[31]

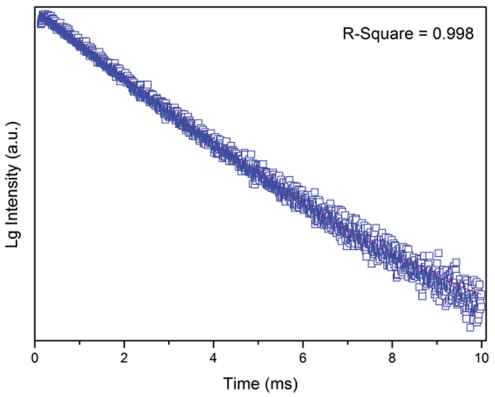

Fig. 5 RT fluorescence decay curve detected at 542 nm (λ_{em} = 276 nm). The solid line represents the best fit to the data.

The RT fluorescence decay curve of the $^5D_4 \rightarrow {}^7F_5$ transitions (542 nm) for the $Na_2Tb_{1.08}Ca_{2.92}Si_6O_{18}H_{0.8}$ phase (Fig. 5) is well fitted by the single exponential function, yielding the lifetime value of τ = 2.498(7) ms, which is in good agreement with the reported value for the Tb^{3+} emission.[32]

4. Implication

Rare earth element-doped chain silicates, such as the $MSiO_3$ (M = Mg, Ca, Sr, Ba) solid solutions, form a very important group of photoluminescence materials, with different M-site cations leading to different photoluminescence spectra.[33–35] Furthermore, there are usually multiple M sites in these silicates. When these M sites are occupied by different rare earth elements, different luminescence properties are resulted in. In the case of the Eu^{2+}-doped $NaScSi_2O_6$–$CaMgSi_2O_6$ solid solutions,[36] as an example, the color-tunable photoluminescence feature was ascribed to the different local M-site environments of the Eu^{2+}. Accordingly, it's important to investigate the rare earth element distribution on the M sites. In this study, we have analyzed the Tb distribution of the chain silicate $Na_2Tb_{1.08}Ca_{2.92}Si_6O_{18}H_{0.8}$ on its different M sites using single-crystal data. Combined with the BVSs, the valences of the Tb have been constrained as well. On the other hand, it remains to be explored whether the structure of this new phase, plus its optical properties, has strong dependence on the substitution between Tb and Ca on the M sites. We believe that the result reported here should stimulate further research on rare earth element-doped silicate photoluminescence materials.

5. Conclusions

In summary, a new microporous compound, with the composition of $Na_2Tb_{1.08}Ca_{2.92}Si_6O_{18}H_{0.8}$ and a novel 3-D framework, has been synthesized under HP conditions. The structure of this phase can be viewed as made of some [MO_6] polyhedron double chains and zigzag [SiO_4] tetrahedron single chains. The [MO_6] polyhedron double chains, in parallel to the *b*-axis, are connected by neighboring SiO_4 tetrahedron *via* vertex oxygen atoms to form a three-dimensional framework. This new phase

contains large 6-membered ring channels along the *b*-axis direction, which are delimited by the [SiO_4] tetrahedra and [MO_6] polyhedra. Its photoluminescence studies are consistent with the crystallographic results, suggesting a strong green emission and a lifetime value of 2.498(7) ms. The successful synthesis of this new terbium silicate under HP conditions and the research on the rare earth element distribution on the M sites will stimulate further study on the lanthanide silicates with novel structures and useful optical properties.

Conflicts of interest

There are no conflicts to declare.

Acknowledgements

This study was financially supported by the Strategic Priority Research Program (B) of Chinese Academy of Sciences (Grant No. XDB18000000), by the DREAM project of MOST, China (Grant No. 2016YFC0600408), and by the Program of the Data Integration and Standardization in the Geological Science and Technology from MOST, China (Grant No. 2013FY1109000-3).

Notes and references

1 D. Ananias, M. Kostova, F. A. A. Paz, A. Ferreira, L. D. Carlos, J. Klinowski and J. Rocha, *J. Am. Chem. Soc.*, 2004, **126**, 10410.
2 G. Wang, J. Li, J. Yu, P. Chen, Q. Pan, H. Song and R. Xu, *Chem. Mater.*, 2006, **18**, 5637.
3 M. Y. Huang, Y. H. Chen, B. C. Chang and K. H. Lii, *Chem. Mater.*, 2005, **17**, 5743.
4 J. Rocha, L. D. Carlos, F. A. A. Paz and D. Ananias, *Chem. Soc. Rev.*, 2011, **40**, 926.
5 D. Ananias, F. A. A. Paz, L. D. Carlos and J. Rocha, *Microporous Mesoporous Mater.*, 2013, **166**, 50.
6 L. D. Sanjeewa, K. Fulle, C. D. McMillen, F. Wang, Y. f. Liu, J. He, J. N. Anker and J. W. Kolis, *Solid State Sci.*, 2015, **48**, 256.
7 D. Ananias, F. A. A. Paz, D. S. Yufit, L. D. Carlos and J. Rocha, *J. Am. Chem. Soc.*, 2015, **137**, 3051.
8 M. Wierzbicka-Wieczorek, M. Göckeritz, U. Kolitsch, C. Lenz and G. Giester, *Eur. J. Inorg. Chem.*, 2015, **2015**, 2426.
9 J. Rocha, P. Ferreira and Z. Lin, *Chem. Commun.*, 1997, **21**, 2103.
10 D. Ananias, A. Ferreira, J. Rocha, P. Ferreira, J. P. Rainho, C. Morais and L. D. Carlos, *J. Am. Chem. Soc.*, 2001, **123**, 5735–5742.
11 A. Ferreira, D. Ananias, L. D. Carlos, C. M. Morais and J. Rocha, *J. Am. Chem. Soc.*, 2003, **125**, 14573.
12 J. Rocha, P. Ferreira, Z. Lin, P. Brandão, A. Ferreira and J. D. P. d. Jesus, *J. Phys. Chem. B*, 1998, **102**, 4739.
13 H. Chen, C. X. Li, Y. J. Hua, L. L. Yu, Q. Y. Jiang, D. G. Deng, S. L. Zhao, H. P. Ma and S. Q. Xu, *Ceram. Int.*, 2014, **40**, 1979.
14 X. G. Zhao, J. Y. Li, P. Chen, Y. Li, Q. X. Chu, X. Y. Liu, J. H. Yu and R. R. Xu, *Inorg. Chem.*, 2010, **49**, 9833.
15 C. Wang, X. Liu, M. E. Fleet, S. Fenga and R. Xua, *J. Solid State Chem.*, 2006, **179**, 2245.
16 C. Wang, X. Liu, M. E. Fleet, J. Li, S. Feng, R. Xu and Z. Jin, *CrystEngComm*, 2010, **12**, 1617.
17 W. Liu, M. Yang, Y. Ji, F. Y. Liu, Y. Wang, X. F. Wang, X. D. Zhao and X. Y. Liu, *RSC Adv.*, 2014, **4**, 26951.
18 W. Liu, Y. Ji, F. Y. Liu, Y. Wang, X. D. Zhao and X. Y. Liu, *RSC Adv.*, 2015, **5**, 29121.
19 L. Chang, X. Liu, C. Wu, X. Liu and G. Li, *Phys. Chem. Miner.*, 2015, **42**, 223.
20 Q. He, X. Liu, B. Li, L. Deng, Z. Chen, X. Liu and H. Wang, *Phys. Chem. Miner.*, 2013, **40**, 29.
21 X. Liu and M. Fleet, *J. Mineral. Petrol. Sci.*, 2009, **104**, 25.
22 J. F. Moulder, W. F. Stickle, P. E. Sobol and K. D. Boomben, *Handbook of X-ray Photoelectron Spectroscopy*, Physical Electronics, 1995.
23 T. K. Hirsch and L. Ojamäe, *Acta Crystallogr., Sect. B: Struct. Sci.*, 2004, **60**, 179.
24 T. K. Hirsch, *Z. Anorg. Allg. Chem.*, 2003, **629**, 666.
25 R. D. Shannon, B. E. Taylor, T. E. Gier, H. Y. Chen and T. Berzins, *Inorg. Chem.*, 1978, **17**, 958.
26 I. D. Brown and D. Altermatt, *Acta Crystallogr., Sect. B: Struct. Sci.*, 1985, **41**, 244.
27 N. E. Brese and M. O'Keeffe, *Acta Crystallogr., Sect. B: Struct. Sci.*, 1991, **47**, 192.
28 P. Dorenbos, *J. Lumin.*, 2000, **91**, 91.
29 P. Dorenbos, *J. Phys.: Condens. Matter*, 2003, **15**, 6249.
30 H. Ebendorff-Heidepriem and D. Ehrt, *Opt. Mater.*, 2002, **18**, 419.
31 G. Blasse, *Prog. Solid State Chem.*, 1988, **18**, 79.
32 W. H. Di, X. J. Wang, B. J. Chen, S. Z. Lu and X. X. Zhao, *J. Phys. Chem. B*, 2005, **109**, 13154.
33 S. H. M. Poort, H. M. Reijnhoudt, H. O. T. Kuip and G. Blasse, *J. Alloys Compd.*, 1996, **241**, 75.
34 Z. G. Cui, G. H. Jia and D. G. Deng, *J. Lumin.*, 2012, **132**, 153.
35 M. A. Mickens and Z. Assefa, *J. Lumin.*, 2014, **145**, 498.
36 Z. G. Xia, Y. Y. Zhang, M. S. Molokeev, V. V. Atuchin and Y. Luo, *Sci. Rep.*, 2013, **3**, 3310.